

Observation of Non-Exponential Orbital Electron Capture Decays of Hydrogen-Like ^{140}Pr and ^{142}Pm Ions

Yu.A. Litvinov^{ab*}, F. Bosch^a, N. Winckler^{ab}, D. Boutin^b, H.G. Essel^a, T. Faestermann^c, H. Geissel^{ab}, S. Hess^a, P. Kienle^{cd}, R. Knöbel^{ab}, C. Kozhuharov^a, J. Kurcewicz^a, L. Maier^c, K. Beckert^a, P. Beller[†], C. Brandau^a, L. Chen^b, C. Dimopoulou^a, B. Fabian^b, A. Fragner^d, E. Haettner^b, M. Hausmann^e, S.A. Litvinov^{ab}, M. Mazzocco^{af}, F. Montes^e, A. Musumarra^{gh}, C. Nociforo^a, F. Nolden^a, W. Plaß^b, A. Prochazka^a, R. Reda^d, R. Reuschl^a, C. Scheidenberger^{ab}, M. Steck^a, T. Stöhlker^{ai}, S. Torilov^j, M. Trassinelli^a, B. Sun^{ak}, H. Weick^a, M. Winkler^a

^aGesellschaft für Schwerionenforschung GSI, 64291 Darmstadt, Germany

^bJustus-Liebig Universität, 35392 Gießen, Germany

^cTechnische Universität München, 85748 Garching, Germany

^dStefan Meyer Institut für subatomare Physik, 1090 Vienna, Austria

^eMichigan State University, East Lansing, Mi 48824, U.S.A.

^fDipartimento di Fisica, INFN, I35131, Padova, Italy

^gINFN-Laboratori Nazionali del Sud, I95123 Catania, Italy

^hUniversità di Catania, I95123 Catania, Italy

ⁱRuprecht-Karls Universität Heidelberg, 69120 Heidelberg, Germany

^jSt. Petersburg State University, 198504 St. Petersburg, Russia

^kPeking University, Beijing 100871, China

We report on time-modulated two-body weak decays observed in the orbital electron capture of hydrogen-like $^{140}\text{Pr}^{59+}$ and $^{142}\text{Pm}^{60+}$ ions coasting in an ion storage ring. Using non-destructive single ion, time-resolved Schottky mass spectrometry we found that the expected exponential decay is modulated in time with a modulation period of about 7 seconds for both systems. Tentatively this observation is attributed to the coherent superposition of finite mass eigenstates of the electron neutrinos from the weak decay into a two-body final state.

1. Introduction

The accelerator facility of GSI Darmstadt with the heavy ion synchrotron SIS coupled via the projectile fragment separator FRS to the cooler-storage ring ESR offers a unique opportunity for decay studies of highly ionized atoms. It is possible to produce, separate, and store for extended

periods of time exotic nuclei with a well-defined number of bound electrons [1]. Basic nuclear properties such as masses and lifetimes are measured by applying the mass- and time-resolved Schottky Mass Spectrometry (SMS) [2,3].

The dependance of β -lifetimes on the atomic charge state q of the parent ion has an obvious impact on our understanding of the processes ongoing in stellar nucleosynthesis [4]. Several successful experiments studying weak decay of highly-

*Corresponding author. E-mail: y.litvinov@gsi.de

[†]25.07.2006 deceased

charged atoms have been performed in the past, e.g., the experimental discovery of bound-state beta decay (β_b) at the example of fully-ionized ^{163}Dy [5]. Due to β_b decay, fully ionized ^{187}Re nuclei decay by 9 orders of magnitude faster than neutral atoms [6]. The first direct measurement of the ratio of bound and continuum β -decay of fully-ionized $^{207}\text{Tl}^{81+}$ was achieved by a direct observation of the decay and growth of the number of parent and daughter ions using SMS [7]. In the course of the present study the first measurements of orbital electron capture (EC) in hydrogen-like (H-like) and helium-like (He-like) ^{140}Pr ions have been performed [8,9]. It was found that the EC decay rate in H-like ^{140}Pr ions is about 50% higher than in He-like ions. This result including the measured EC/ β^+ branching ratios can be explained by standard weak decay theory [10,11].

The change of the mass manifests a radioactive decay and is evidenced by a corresponding correlated change of the revolution frequency. The area of the Schottky frequency peak is proportional to the number of stored ions and to the square of the atomic charge state, q^2 . The SMS is sensitive to *single* stored ions with atomic charge states $q \geq 30$ [3]. However, due to a large variance in determination of the peak areas, it became apparent that only by restricting to *three* injected parent ions at maximum one could exclude any uncertainty in the determination of the *exact* number of circulating ions. With this constraint the time of the decay of each stored ion can be precisely determined. On this basis single particle decay-spectroscopy has been developed which allows for an unambiguous and background-free identification of a certain decay branch [8,12]. This leads, however, to a very laborious collection of data which requires at least some thousand measurements to get a statistically reasonable number of decays.

Here we report on the first experiments which used time-resolved single-particle decay spectroscopy for studying the time evolution of two-body weak decays, i.e. EC and β_b -decays of radioactive ions in the ESR. The physics motivation was the question whether or not the electron neutrinos generated in such decays as coherent superposition of mass eigenstates would affect the

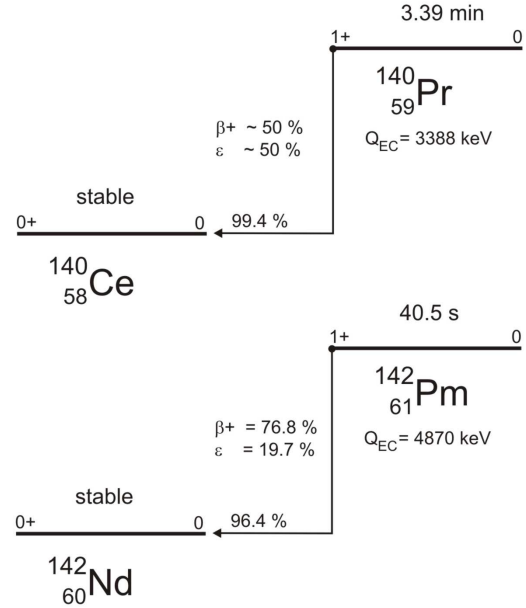


Figure 1. Decay schemes of neutral ^{140}Pr (upper panel) and ^{142}Pm (lower panel) atoms [14].

exponential decay [13]. H-like ^{140}Pr and ^{142}Pm ions have been selected for these studies. Both nuclei decay to stable daughter nuclei via either the three-body positron emission or the two-body EC-decay. Well-known decay schemes of neutral ^{140}Pr and ^{142}Pm atoms [14] are illustrated in Figure 1. Both systems decay mainly by a single allowed Gamow-Teller ($1^+ \rightarrow 0^+$) transition. The weak transitions to excited states can be safely neglected in our context. These nuclides have quite different decay energies (Q_{EC} values) and lifetimes, thus allowing a detailed comparison of the time evolution of the decays with different Q_{EC} and lifetimes. Both Q_{EC} -values are sufficiently large to be easily resolved by SMS. Furthermore, their half-lives are much larger than the time needed for the preparation of the ions.

2. Experiment

H-like $^{140}\text{Pr}^{58+}$ and $^{142}\text{Pm}^{60+}$ ions were produced by fragmentation of primary beams of ^{152}Sm fast extracted from the SIS with energies in the range between 500-600 MeV per nucleon. The duration of the extraction pulse was less than 1 μsec which is essential since we require a well-defined time of the creation of the ions. Beryllium production targets placed at the entrance of the FRS with thicknesses of 1 and 2 g/cm^2 have been applied. The important parameters used for the experiment are summarized in Table 1. Three independent experiments were performed with Pr ions (runs 1,2 and 3) and one with Pm ions (run 4) for comparison.

The fragments of interest were separated in-flight with the FRS using the $B\rho\text{-}\Delta E\text{-}B\rho$ method [15]. For this purpose, a 731 mg/cm^2 aluminum degrader was inserted at the middle focal plane of the FRS. In runs 3 and 4 a 256 μm niobium foil after the degrader has been used in addition. In this way we separated $^{140}\text{Pr}^{58+}$ and $^{142}\text{Pm}^{60+}$ fragments without isobaric contaminations at the exit of the FRS. More details on the separation of pure $^{140}\text{Pr}^{58+}$ ions in these experiments can be found in Ref. [12].

Single bunches (less than 1 μs long) of separated ions containing on the average only two parent ions were injected into the ESR at the injection energy of 400 MeV per nucleon and then stored in the ultrahigh vacuum ($\sim 10^{-11}$ mbar). Their velocity spread caused by the production reaction was reduced within 6-10 sec first by stochastic pre-cooling [16] and then by electron cooling [17] to a value of $\Delta v/v \approx 5 \cdot 10^{-7}$. The ions coasted in the ring with a velocity of 71% of the speed of light, corresponding to a relativistic Lorentz factor of 1.43.

The 30th harmonics of the revolution frequency f of about 2 MHz (circumference of the ring is 108.3 m) was measured by the Fourier frequency analysis of the signals induced by the coasting ions at each revolution in pick-up plates. For cooled ions f is uniquely related to the mass-overcharge ratio M/q of the stored ions, which is the basis for the Schottky mass measurements [18]. Thus the ions of interest and their decay prod-

ucts could be unambiguously identified.

The data were acquired with the commercial realtime spectrum analyzer Sony-Tektronix 3066. It was triggered with the logic signal corresponding to the start event of the injection kicker of the ESR. After each trigger event, the analyzer was recording a given number of Fourier transformed noise power spectra - FFT (Fast Fourier Transform) frames. Each FFT frame had a bandwidth of 5 kHz and was collected for 128 msec. Each subsequent frame was started after a defined delay of 64 msec (runs 1, 3 and 4) or 50 msec (run 2). The recorded data were automatically stored on disk for off-line analysis.

In the ESR, the transition from the parent to the daughter ion in a nuclear decay is evidenced by a well-defined change Δf of the revolution frequency. Thus, by keeping the number of coasting ions small we could *continuously* monitor the "mass" of each ion in time and determine precisely its decay time. In our case the parent ions could have three possible fates, namely EC or β^+ -decay or a loss due to atomic charge exchange reactions.

Since the atomic charge state q does *not* change in the EC-decay, Δf is determined by the mass difference (Q_{EC} -value) between the parent and daughter nuclei. The corresponding change in the revolution frequency is a few hundred Hz only (about 270 Hz for the case of ^{140}Pr and about 310 Hz for the case of ^{142}Pm) (30th harmonics). The decay is characterized by the *correlated* disappearance of the parent ion and appearance of the daughter ion. The appearance in the frequency spectrum is delayed by about 900 ± 300 msec needed to cool the recoiling daughter ions. Their kinetic energies are 44 eV and 90 eV (c.m.) for the cases of ^{140}Ce and ^{142}Nd daughter nuclei, respectively. The ESR lattice and the applied ion-optical setting guarantee that *all* recoil ions still remain in the acceptance irrespective on the direction of their emission.

In β^+ -decay the atomic charge changes by one unit and the frequency of the corresponding daughter ion is shifted by about -150 kHz (30th harmonics). This frequency shift is by far larger than our small observation band, and the decay is only seen by a decrease of the number of the

parent ions. Such a disappearance, however, cannot be distinguished from the loss of the ion due to atomic capture or loss of an electron by reactions with the atoms of the residual gas or the electrons of the cooler. However, from the losses observed for the stable daughter ions a loss constant $\lambda_{loss} \leq 2 \cdot 10^{-4} \text{ sec}^{-1}$ (the loss constants for H-like parent ions and fully-ionized daughter ions are almost the same [7]) could be extracted which is at least one order of magnitude smaller than the EC and β^+ decay constants λ_{EC} and λ_{β^+} , respectively. We also note that mechanical scrapers of the ESR were positioned to remove the decay products of the atomic charge-exchange reactions and the β^+ -decay daughter ions.

Two out of many thousand runs are illustrated in Figure 2 as a water-flow diagram starting at the time of the injection into the ring. These examples show one (upper panel) and two (lower panel) injected parent ions. Each horizontal line represents a frequency spectrum with 8 Hz/channel averaged over five consecutive FFT frames. The first several seconds are needed for the combined stochastic and electron cooling. The decay times are clearly seen. We emphasize that such a *continuous* observation of both the parent and daughter ions *excludes* any possible time-dependent alteration of the detection efficiency.

3. Data analysis and results

The aim of the analysis was to study precisely the decay characteristics of each EC-decaying ion. For this purpose, at least two independent visual and one automatic analysis have been applied to the data of each experimental runs.

For achieving a better signal-to-noise ratio one may average several subsequent Schottky spectra as it is done in Figure 2. In this way, however, one reduces the time resolution. In the visual analysis we analyzed the un-averaged FFT frames or the average over two subsequent frames. For the automatic analysis we had to average 5 FFT frames in order to achieve a sufficient signal-to-noise ratio. The details of the automatic data evaluation are described in Refs. [19,20].

The analysis was done by inspection of each FFT spectrum taken as a function of time. Then

the time of appearance of a daughter nucleus following the decay of its mother was determined. It was demanded that the decay times determined in independent analysis agree within less than one second. Only the times of the appearance of the daughter nuclei were considered, which are delayed compared to the decay of the mother ion by about 900 ± 300 msec.

The decay times from the three runs with H-like ^{140}Pr were combined. These results and the results for ^{142}Pm ions are illustrated in Figure 3 and in Figures 4 and 5, respectively. The time of the injection into the ESR is within $1 \mu\text{s}$ the time of the creation of the ions. The data were fitted with the exponential decay function:

$$\frac{dN_{EC}(t)}{dt} = N(0) \cdot \lambda_{EC} \cdot e^{-\lambda t}, \quad (1)$$

where $N(0)$ is the number of parent ions at the time $t = 0$, the time of injection and $\lambda = \lambda_{EC} + \lambda_{\beta^+} + \lambda_{loss}$. The ratio of $\lambda_{EC}/\lambda_{\beta^+}$ is 0.95(8) for the H-like ^{140}Pr and is expected to be about 0.32 for the H-like ^{142}Pm [9].

It is clear to see that the expected exponential decrease of the EC-decays as a function of time shows a superimposed periodic time modulation. To account for this modulation we fitted the data with the function:

$$\frac{dN_{EC}(t)}{dt} = N(0) \cdot e^{-\lambda t} \cdot \widetilde{\lambda}_{EC}(t), \quad (2)$$

where $\widetilde{\lambda}_{EC}(t) = \lambda_{EC} \cdot [1 + a \cdot \cos(\omega t + \phi)]$ with an amplitude a , an angular frequency ω , and a phase ϕ of the modulation. For the case of ^{142}Pm ions only the first 33 seconds after the injection were fitted with Eq. 2 due to the short half-life of the mother nuclei and, thus, the fast damping of the modulation amplitude.

The fits were done with the MINUIT package [21] using the χ^2 minimization and the maximum likelihood methods which yielded consistent results. The fit parameters are given in Table 2.

From the angular frequency ω of Table 2 we can extract the periods of the modulation of 7.06(8) sec and 7.10(22) sec (laboratory frame) for ^{140}Pr and ^{142}Pm ions, respectively. The presence of the modulation frequencies was also confirmed by Fast Fourier Transforms (see insets in

Figure 3 and Figure 4). The amplitudes a agree within the error bars. The average value of both systems is $\langle a \rangle = 0.20(2)$.

4. Discussion

The observed periodic modulations of the expected exponential decrease of the number of EC-decays per time unit still suffer from restricted statistics. However, the "zero hypothesis" of a pure exponential decay can be already rejected according to the χ^2/DoF -values from Table 2 on the 99% confidence level (one-sided probabilities $p = 0.006$) for both investigated nuclear systems.

First of all, the finding of nearly the same oscillation period of about 7 sec might suggest a technical artefact as their common origin, such as periodic instabilities in the storage ring or of the recording systems. However, this explanation is very improbable due to our detection technique where we have—during the whole observation time—the *complete and uninterrupted information upon the status of each stored ion*. Furthermore, the parent and daughter ions from both systems coast on different orbits in the ESR and have different circulation times. We can also exclude binning effects or the variance of the delay between the decay of the mother and the "re-appearance" of the daughter ion, since these effects lead to an uncertainty of the decay time that is much smaller than the observed period.

It is very probable that the H-like ^{140}Pr as well as the ^{142}Pm ions with nuclear spin $I = 1^+$ are produced in a coherent superposition of the two $1s$ hyperfine states with total angular momenta $F = 1/2$ and $F = 3/2$. This could lead to well-known quantum beats with a beat period $T = h/\Delta E$, where ΔE is the hyperfine splitting. However, those beat periods should be more than twelve orders of magnitude shorter than the observed ones.

The weak decay conserves the F quantum number, and since the final state (fully ionized daughter nuclei with $I = 0^+$ and emitted electron neutrino ν_e) has $F = 1/2$, the EC-decay from the $F = 3/2$ state is *not* allowed [8,9]. Only a hypothetical, yet unknown, mechanism which transfers the parent ions periodically within 7 seconds

from the $F = 1/2$ ground state to the $F = 3/2$ state and back in both nuclides could generate the observed modulations [22].

Thus, we try to interpret the modulations as due to the properties of the electron neutrino that is generated in the EC-decay as a coherent superposition of at least two mass eigenstates. This necessarily comprises that also the recoiling daughter nuclei appear as a coherent superposition of states that are entangled with the electron neutrino mass eigenstates by momentum- and energy conservation.

We note that a time structure was observed in the two-body decay of stopped pions in KARMEN experiment (KARMEN time anomaly) [23]. This anomaly was described in Ref. [24] by using a function containing periodic time modulation similar to Eq. 2.

There is a long-lasting and still persisting debate whether the generated neutrino mass eigenstates should have the same energy or rather the same three-momentum \vec{q}_ν or neither of them [25,26,27,28,29]. In our case, this question can be addressed properly only in the context of wave-packets since we observe the decaying system in a restricted region of space and time. This necessarily generates an uncertainty of both momentum and energy. An attempt to interpret the modulation times in this framework has been made in Ref. [30].

Disregarding momentum and energy spread in a simplified picture and restricting to two neutrino mass eigenstates, one gets from momentum and energy conservation for an initial state with energy E and momentum $P = 0$ in the c.m. system³:

$$E_1 + M + \frac{p_1^2}{2M} = E \quad (3)$$

$$E_2 + M + \frac{p_2^2}{2M} = E, \quad (4)$$

where $E_i = \sqrt{p_i^2 + m_i^2}$ denotes the energy of the two neutrino mass eigenstates with masses m_1 and m_2 , respectively, $p_i^2/2M$ the corresponding kinetic energies of the recoiling daughter nuclei, and where M is the mass of the daughter nucleus.

³In the following we set $c=1$.

By combining these two equations and neglecting a term given by the ratio of the recoil energy and the mass of the daughter nucleus we arrive at (see e.g. Ref. [31,32]):

$$\Delta E = E_2 - E_1 \approx \frac{\Delta m^2}{2M}, \quad (5)$$

where $\Delta m^2 = m_1^2 - m_2^2$.

The modulations could be caused by the energy splitting ΔE which is indicated by almost the same observed modulation periods for both decaying nuclei ^{140}Pr and ^{142}Pm with almost the same nuclear masses M but with quite different neutrino energies and, thus, momenta. One expects for a mass of 140 mass units and for $\Delta m^2 \approx 10^{-4} \text{ eV}^2$ [33] a period in the c.m. system of roughly $T=10$ sec. Besides the fact that this estimate is based on several assumptions many questions remain. How could the coherence of the entangled quantum states be preserved over time spans of some ten seconds? What is the effect of the continuous monitoring of the state of the ion? Is the "phase" between the entangled neutrino mass eigenstates set back to zero at each observation?

It is obvious that our findings must be corroborated by the study of other two-body beta decays (EC and β_b). Furthermore, it has to be investigated how the oscillation period—if persisting at all—depends on the nuclear mass M . Mandatory are also investigations of three-body β -decays, where oscillations should be washed out due to the broad distribution of neutrino (sc. recoil) energies. Finally, an interesting case arises when the decaying nucleus is not free, but couples to the full phonon spectrum in the lattice of a solid.

Acknowledgements

We would like to express our deep gratitude to W. Henning for his continuous support and invaluable advice. It is a pleasure to acknowledge many fruitful and engaged discussions with L. Batist, K. Blaum, P. Braun-Munzinger, H. Emling, A. Fäßler, B. Franzke, S.J. Freedman, L. Grigorenko, A. Ivanov, H.-J. Kluge, E. Kolomeitsev, R. Krücken, K. Lind-

ner, M. Lindroth, G. Münzenberg, Z. Patyk, K. Riisager, A. Schäfer, J. Schiffer, D. Schwalm, R. Schuch, N. Severijns, H. Stöcker, P.M. Walker, J. Wambach, and H. Wilschut. We would like to thank in particular H. Feldmeier, M. Kleber, K.H. Langanke, H. Lipkin, P. Vogel, Ch. Weinheimer, and K. Yazaki for intensive theoretical discussions. We are grateful to Th. Müller and A. Le Fèvre for the help in the data evaluation. We are indebted to the HADES and IKAR collaborations for their help and flexibility concerning the beam time schedule. The excellent support by the accelerator team of GSI decisively contributed to the successful achievement of our experiments. One of us (M.T.) acknowledges the support by the A. von Humboldt Foundation.

REFERENCES

1. H. Geissel et al., Phys. Rev. Lett. **68** (1992) 3412.
2. T. Radon et al., Phys. Rev. Lett. **78** (1997) 4701.
3. Yu.A. Litvinov et al., Nucl. Phys. **A 756** (2005) 3.
4. K. Takahashi and K. Yokoi, Nucl. Phys. **A 404** (1983) 578.
5. M. Jung et al., Phys. Rev. Lett. **69** (1992) 2164.
6. F. Bosch et al., Phys. Rev. Lett. **77** (1996) 5190.
7. T. Ohtsubo et al., Phys. Rev. Lett. **95** (2005) 052501.
8. H. Geissel et al., Eur. Phys. J., Special Topics **150** (2007) 109.
9. Yu.A. Litvinov et al., Phys. Rev. Lett. **99** (2007) 262501.
10. Z. Patyk et al., Phys. Rev. **C 77** (2008) 014306.
11. A.N. Ivanov, M. Faber, R. Reda, and P. Kienle, Phys. Lett. B, *in press* (2008); *arXiv:nucl-th/0711.3184*.
12. Yu.A. Litvinov et al., *arXiv:nucl-ex/0509019*.
13. Yu.A. Litvinov, F. Bosch, et al., Experimental proposal for SIS-FRS-ESR facilities E077, GSI, Darmstadt, 2006.
14. R.B. Firestone et al., *Table of Isotopes*, 8th Edition, Wiley, New York, 1999.

15. H. Geissel et al., Nucl. Instr. and Meth. **B 70** (1992) 286.
16. F. Nolden et al., Nucl. Instr. and Meth. **A 532** (2004) 329.
17. M. Steck et al., Nucl. Instr. Meth. **A 532** (2004) 357.
18. T. Radon et al., Nucl. Phys. **A 677** (2000) 75.
19. H.G. Essel, GSI Scientific Report 2006, GSI Report 2007-1 (2007) p. 205.
20. N. Winckler, Doctoral Thesis, JLU Giessen, in preparation.
21. *Function Minimization and Error Analysis* (MINUIT), CERN Program Library, Computing and Network Division, CERN Geneva, Switzerland; <http://wwwasdoc.cern.ch/wwwasdoc/minuit/minmain.html>.
22. Ch. Weinheimer, L. Grigorenko and E. Kolomeitsev, private communications (2007).
23. B. Armbruster et al., Phys. Lett. **B 348** (1995) 19.
24. Y.N. Srivastava, et al., *arXiv:hep-ph/9807543* (1998).
25. S. Bilenky and B. Pontecorvo, Phys. Rep. **41C** (1978) 225.
26. B. Kayser, Phys. Rev. **D 24** (1981) 110.
27. A.D. Dolgov, A.Yu. Morozov, L.B. Okun, and M.G. Schepkin, Nucl. Phys. **B 502** (1997) 3.
28. L. Stodolsky, Phys. Rev. **D 58** (1998) 036006.
29. H.J. Lipkin, Phys. Lett. **B 579** (2004) 355.
30. A.N. Ivanov, R. Reda, and P. Kienle, *to be published*.
31. J. Lowe et al., *arXiv:hep-ph/9605234v2*.
32. Y. Srivastava, A. Widom, and E. Sassaroli, Eur. Phys. J. **C 2** (1998) 769.
33. The KamLAND Collaboration, Phys. Rev. Lett. **94** (2005) 081801.

Table 1

Primary beam, target and degrader parameters, number of measurements. Each line represents a different experimental run labelled in the first column. The ion of interest is given in the second column. Energy of the ^{152}Sm primary beam $E(^{152}\text{Sm})$ and the thickness of the beryllium production target $L(^9\text{Be})$ are given in the third and fourth columns, respectively. The number of measurements performed in each run $\#_{inj}$ is given in the last column.

run	ion	$E(^{152}\text{Sm})$ [MeV/u]	$L(^9\text{Be})$ [mg/cm ²]	$\#_{inj}$
1	$^{140}\text{Pr}^{58+}$	507.8	1032	453
2	$^{140}\text{Pr}^{58+}$	507.8	1032	842
3	$^{140}\text{Pr}^{58+}$	601.1	2513	5807
4	$^{142}\text{Pm}^{60+}$	607.4	2513	7011

Table 2

The fit parameters obtained for ^{140}Pr (upper part) and ^{142}Pm (lower part) EC-decay data illustrated in Figures 3, 4 and 5. The fits are done according to Eq. 1 and Eq. 2 which is indicated in the first column. The corresponding χ^2/DoF (DoF = degrees of freedom) are given in the last column.

Fit parameters of ^{140}Pr data					
Eq.	$N_0\lambda_{EC}$	λ	a	ω	χ^2/DoF
1	34.9(18)	0.00138(10)	-	-	107.2/73
2	35.4(18)	0.00147(10)	0.18(3)	0.89(1)	67.18/70
Fit parameters of ^{142}Pm data					
Eq.	$N_0\lambda_{EC}$	λ	a	ω	χ^2/DoF
1	46.8(40)	0.0240(42)	-	-	63.77/38
2	46.0(39)	0.0224(41)	0.23(4)	0.89(3)	31.82/35

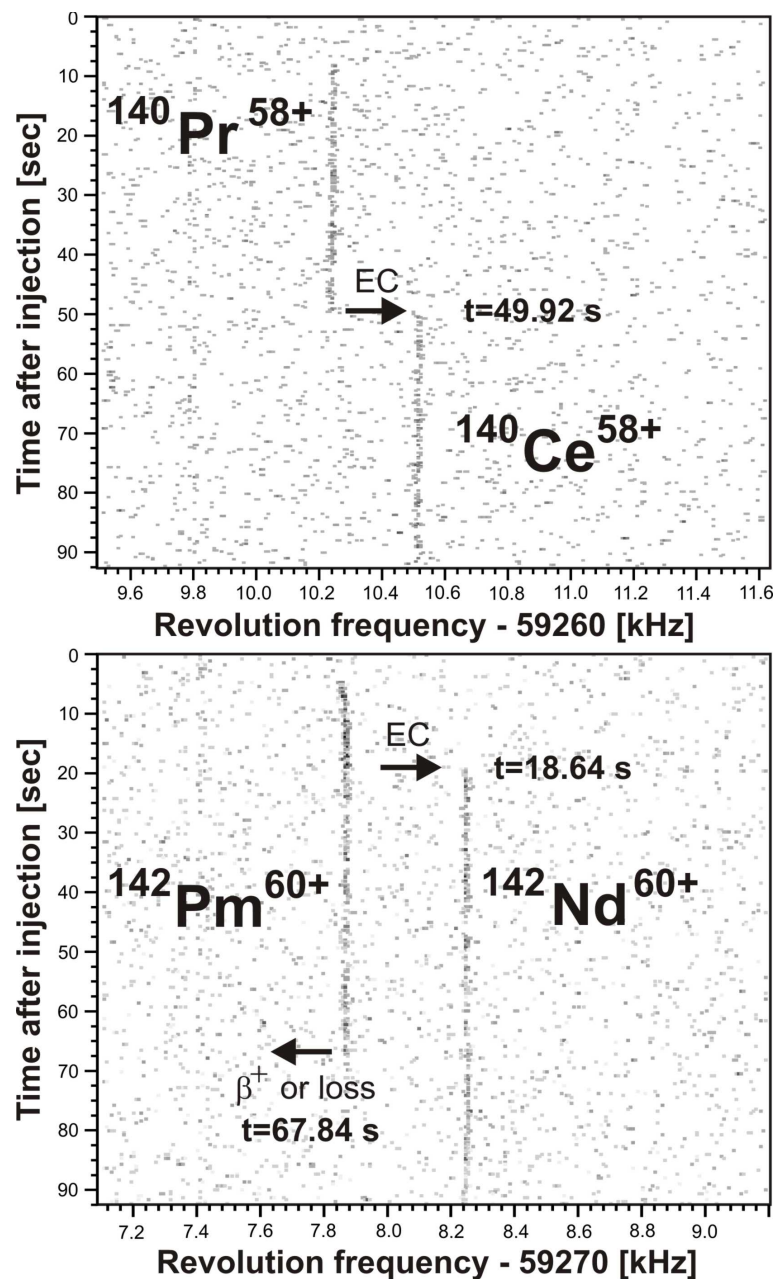


Figure 2. Upper panel: a series of consecutive frequency spectra of a single parent $^{140}\text{Pr}^{58+}$ ion decaying to the daughter $^{140}\text{Ce}^{58+}$ ion 49.92 sec after the injection into the ESR. Lower panel: two injected $^{142}\text{Pm}^{60+}$ ions decay 18.64 sec and 67.84 sec after the injection. The first ion decays by electron capture to a $^{142}\text{Nd}^{60+}$ ion. The second ion decays by β^+ -decay or is lost due to atomic charge exchange reactions. The times of the correlated disappearance of the parent ions and the appearances of EC-daughter ions are clearly seen. The first few seconds are needed for cooling. The frequency differences between parent and daughter ions correspond to Q_{EC} values of 3.35 MeV and 4.83 MeV for $^{140}\text{Pr}^{58+}$ and $^{142}\text{Pm}^{60+}$ ions, respectively.

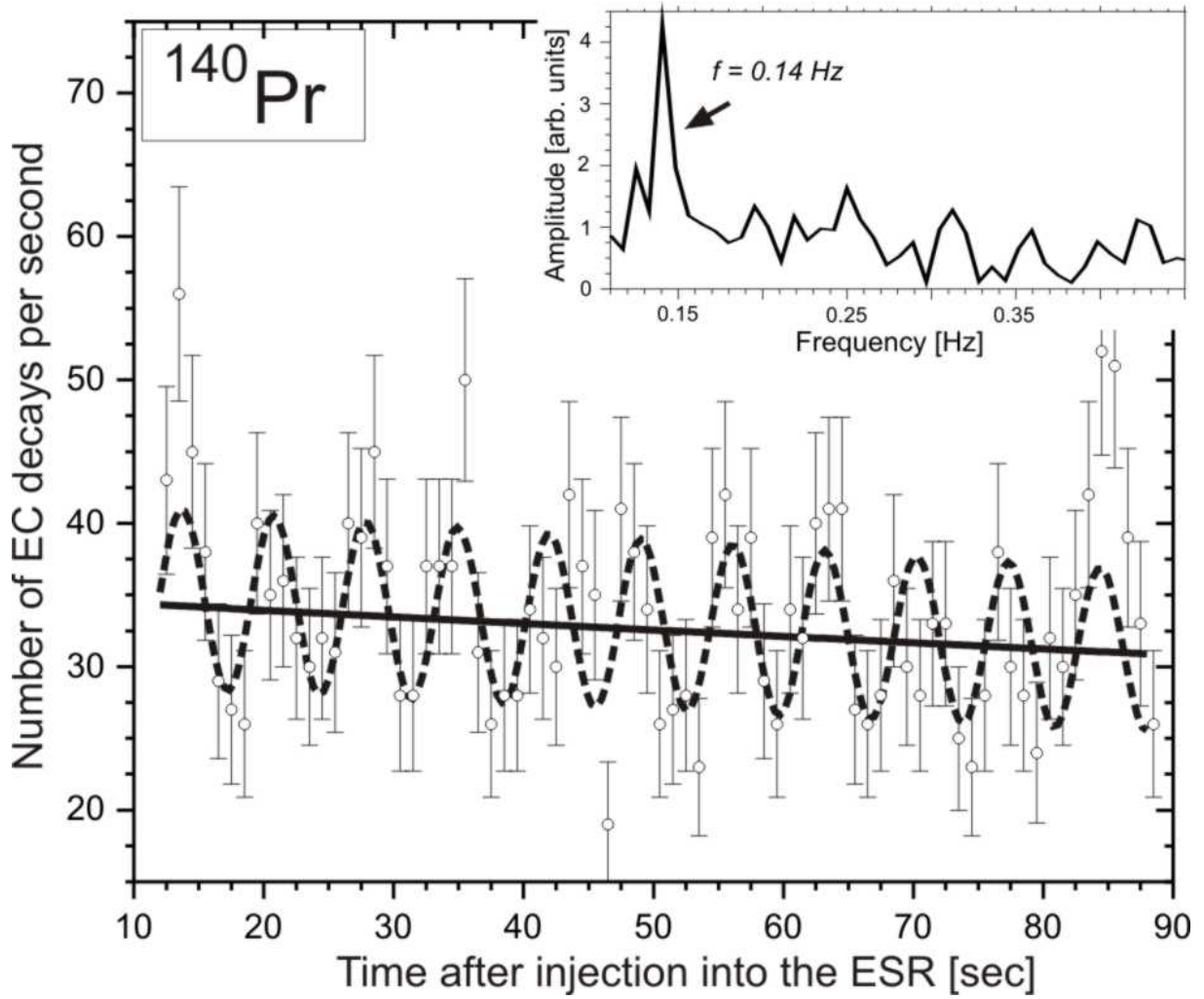


Figure 3. Number of EC-decays of H-like ^{140}Pr ions per second as a function of the time after the injection into the ring. The solid and dashed lines represent the fits according to Eq. 1 (without modulation) and Eq. 2 (with modulation), respectively. The inset shows the Fast Fourier Transform of these data. A clear frequency signal is observed at 0.14 Hz (laboratory frame).

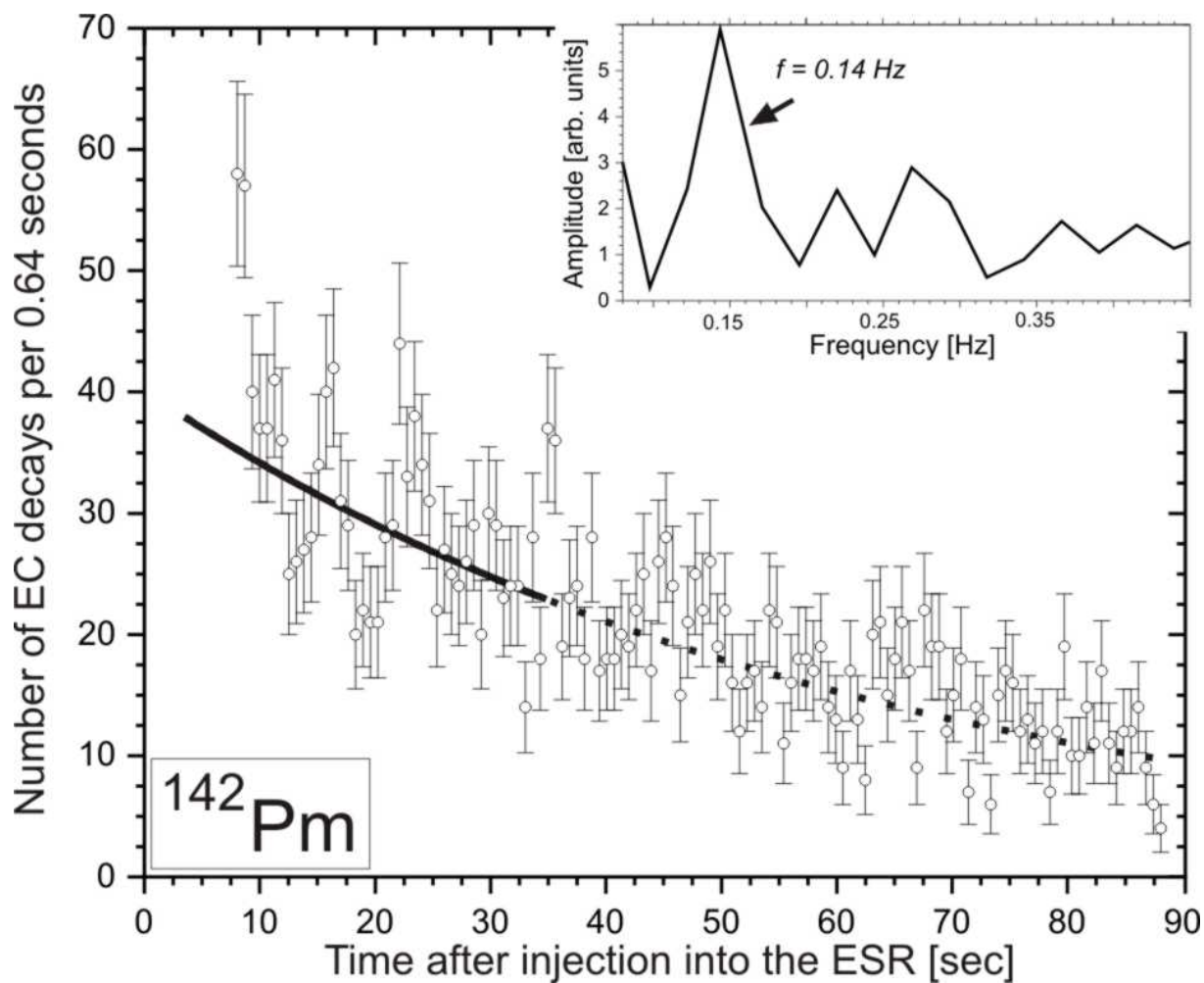


Figure 4. Number of EC-decays of H-like ^{142}Pm ions per 0.64 seconds as a function of the time after the injection into the ring. The solid line represents the exponential decay fit according to Eq. 1 until 33 sec after injection (continued as a dotted line). The inset shows the FFT spectrum obtained from the data until 33 sec. The reduced resolution compared to Figure 3 is explained by a smaller number of points used for the FFT. A clear FFT peak is observed at about 0.14 Hz (laboratory frame).

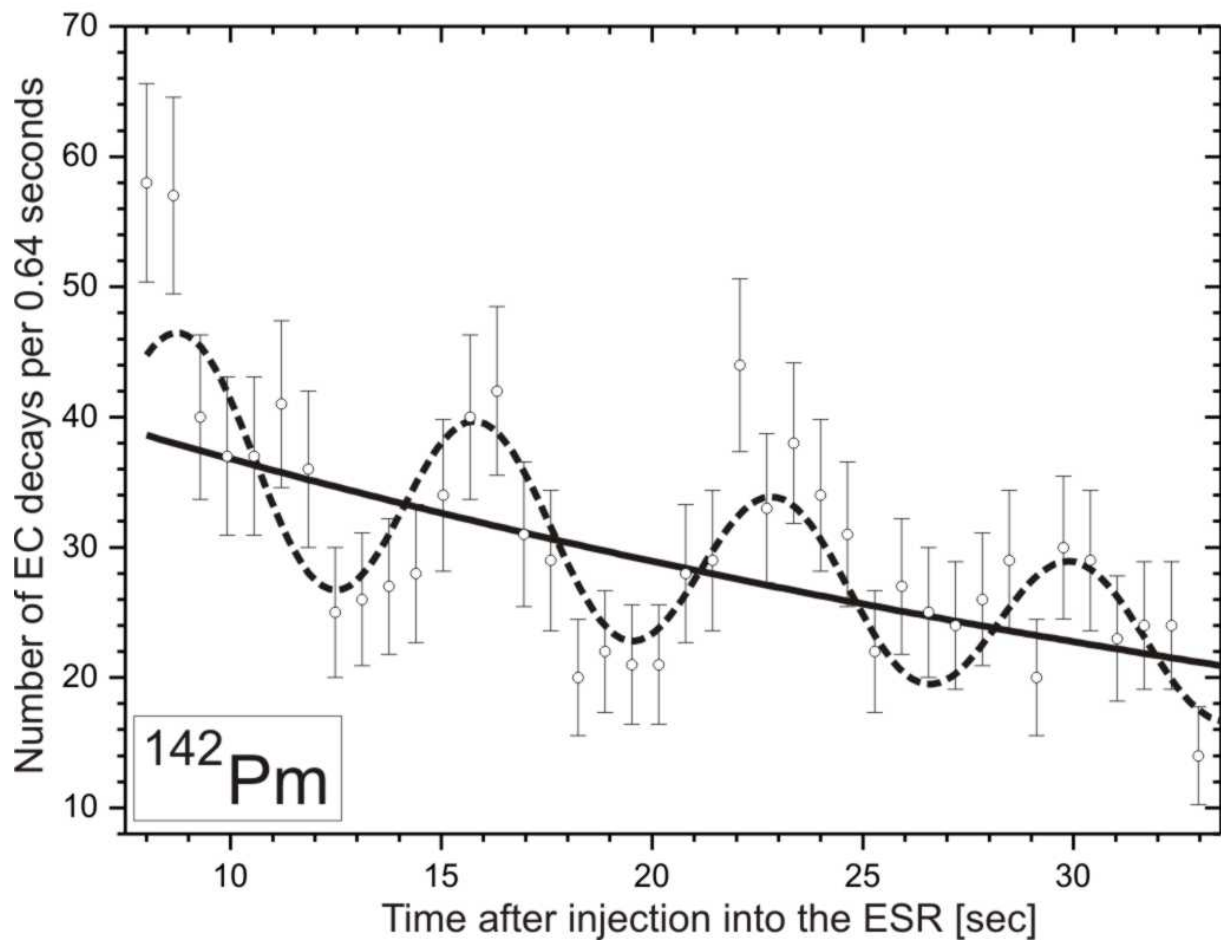


Figure 5. A zoom to the first 33 sec after injection of the data presented in Figure 4. The solid line represents the exponential decay fit according to Eq. 1. The dashed line shows the fit according to Eq. 2.